Cracking behavior of Sea Sand RC Beam Bonded Externally with CFRP Plate

Amin Al-Fakih [a,b*], Mohd Hisbany Mohd Hashim [c], Rayed Alyousef [d], Ayad Mutafi [e], Saddam Hussein Abo Sabah [f], and T. Tafsirojjaman [g]

[a] Department of Civil and Environmental Engineering, Universiti Teknologi PETRONAS (UTP), 32610 Bandar Seri Iskandar, Perak, Malaysia
[b] College of Civil Engineering, Fuzhou University, Fuzhou 350108, China
[c] School of Civil Engineering, Faculty of Engineering, Universiti Teknologi MARA, 40450 Shah Alam, Selangor, Malaysia
[d] Department of Civil Engineering, College of Engineering in Al-Kharj, Prince Sattam Bin Abdulaziz University, Al-Kharj 16273, Saudi Arabia
[e] Department of Aerospace Engineering, Universiti Putra Malaysia, Selangor 43400, Malaysia
[f] Jamilus Research Centre for Sustainable Construction (JRC), Faculty of Civil Engineering and Environmental Engineering, Universiti Tun Hussein Onn Malaysia, Parit Raja 86400, Johor, Malaysia
[g] Centre for Future Materials (CFM), School of Civil Engineering and Surveying, University of Southern Queensland, Toowoomba, QLD 4350, Australia

[*] Correspondence: amin.ali_g03663@utp.edu.my

Abstract

CFRP is an alternative technique for cracking control of high-chloride reinforced concrete (RC) beams. This research, therefore, investigates the strength performance and failure mode and cracking behaviour of RC beams incorporated with sea sand bonded externally with the carbon fibre reinforced polymer (CFRP) plate. Sea sand is used as a 100% replacement of fine aggregate. Three batches of RC beams were carried out in this research, including the control beam (no sea sand neither CFRP), RC beam with normal sand bonded with CFRP plate, and RC beam with sea sand and bonded with CFRP. A four-point bending test was performed under static loading for the specimens. Finite element simulation was modelled for further comparison. The experimental findings showed that the flexural capacity of the sea sand RC beam bonded externally with CFRP plate is 5.50% greater than the flexural strength of the beam without CFRP (control beam). Besides, results demonstrated that RC beams bonded externally with CFRP were failed by plate end debonding (PED) while the control RC beam without bonding was failed at the mid-span by concrete crushing. However, the bonded RC beams were stiffer, which could lead to

lower crack spacing. Finite element simulation showed very acceptable results compared to the experimental results.

Keywords: Cracking patterns; Sea sand concrete; Flexural strength; CFRP; Finite element simulation

1. Introduction

A new form of concrete called "sea sand concrete" is a form that uses sea sand as a fine aggregate that, in recent years, has wide applications in the coastal zones [1]. Sea sand addresses the shortage of river sand and blends it with lower costs, as most ready-mixed firms use sea sand rather than standard sand even without treatment [2, 3]. The use of sea sand as an alternative for normal sand would be considered as a resource that provides sustainability to nature and enhances the mechanical characteristics of concrete [4]. A comprehensive review of the advantages of utilizing sea sand in concrete was carried out by Dhondy, et al. [4] and Xiao, et al. [5], concluding that most researchers have discovered comparable, if not better, mechanical characteristics of sea sand concrete than traditional concrete. They have found that sea sand concrete possesses/gets high early strength and higher compressive strengths compared to standard concrete.

The salt content is the primary distinction between sea sand and normal sand. However, the internal steel bars undergo accelerated corrosion when sea sands aggregate, which comprises a wide range of chlorides, are utilized in concrete. Thus, before sea sand is used in concrete, chloride ions must be removed, which raises costs and risks [3]. Instead of eliminating chloride ions from the sea sand aggregate, researchers have proposed the utilization of fibre reinforced polymers (FRP) plates/sheets/meshes, which consider as non-corrosive material, as a solution [4-15]. Studies reported that the structures of fibre reinforced sea sand concrete is most desirable for the development of infrastructure in areas with restricted access to normal sand and freshwater but convenient access to sea sand and sea-water (e.g., offshore and coastal areas) [16]. Dong, et al. [3] have reinforced the sea-water sea sand coral concrete (Coral-SWSSC) beams with basalt fibre reinforced polymer (BFRP) bars. Authors replaced the top of the Coral-SWSSC beams with ultrahigh-performance concrete (UHPC) and replaced the longitudinal reinforcement bars and stirrups with BRRP bars as well as strengthened the tension face of the beam with BFRP wrapped steel tube (tensile reinforcement). The findings revealed a considerable

high enhancement in the ultimate bending capacity and displacement, energy absorption, and bending stiffness of the developed beams in comparison with the control.

Meikandaan and Murthy [17] have investigated the efficiency of CFRP laminates to repair concrete damaged beams. They found that CFRP laminates enhanced the ultimate load carrying capacity of the strengthened beams by 17 % compared to that of the control beam. It also delayed the initiation of cracks. Remennikov et al. [18] have also externally bonded CFRP sheets to concrete beams and noticed an increase of 28.5% in the load capacity. CFRP sheets were also used to improve the performance of prestressed concrete beams by Wight et al. [19]. The findings were that CFRP reduced the strain in the reinforcements, delayed the reinforcement yielding, and significantly increased the ultimate strength of concrete beams. Furthermore, Hosny et al. [20] and Grace et al. [21] have reported that CFRP contributed greatly to the enhancement of the beam ultimate carrying capacity. Grace et al. [21] have also indicated that the use of CFRP reduced deflections and cracks that do occur are smaller and more evenly distributed.

Therefore, utilization of fibre-reinforced polymer (FRP) in civil and structural engineering applications has become very common around the world, due to its most remarkable advantages, including high resistance to corrosion, substantial improvement in the strength and stiffness of an established structural element with minimal impact on the environment, and high strength to weight ratio [22-28]. Therefore, a researcher claimed that when FRPs (carbon, glass, aramid, and basalt fibre) are utilized as concrete strengthening materials, sea sand can be utilized without even salt removal [3]. The failure modes or FRP retrofitted beams have been examined and observed the interfacial debonding and FRP sheet rupture as the main failure mode [29, 30]. Typically, the utilization of composite fibre plates like CFRP removes the risk of epoxy-platform corrosion and decreases the probability of bonding failure. However, various modes of failure for RC beams bonded externally with CFRP plates are illustrated in Fig. 1. These modes of failure are “flexural failure by FRP fracture, flexural failure by crushing of compressive concrete, critical diagonal crack (CDC), shear failure, plate end interfacial debonding, concrete cover separation, and intermediate crack (IC) induced interfacial debonding” [15, 31-33].

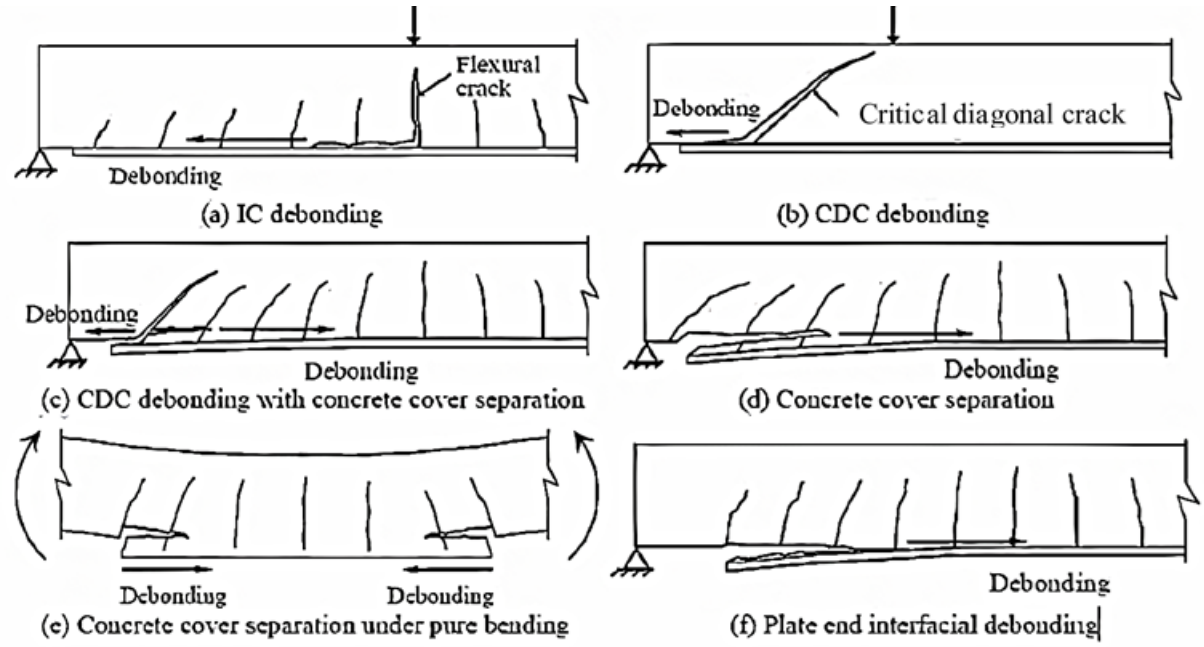

Fig. 1. Typical modes of Failure of RC beams bonded externally with FRP plate [32, 33]

RC structures externally attached to polymer composites are massively complicated in terms of cracking behaviour patterns. As well as transferring stress between steel bars and concrete, the transfers from the exterior plate to concrete must be taken into consideration, depending on the bonding laws of the interface. Previous studies have reported that RC beams externally bonded to CFRP and exposed to the wet and dry environment under sea-water exposure have decreased their strength by 33 percent [34].

The failure position along the beam and detached concrete thickness depends mainly on crack patterns and load arrangements [35]. Therefore, RC beam cracking control is typically attained by limiting the stress increase in the bonded reinforcement and confirming that the bonded reinforcement is appropriately distributed. Still, this way of cracking control is not sufficient enough for high chloride RC beams, which allow for corrosion of the bonded reinforcement and lead to high cracking propagation and low bending and shear resistance. In this respect, another tool for cracking control of high-chloride RC beams is carbon fibre reinforced polymer (CFRP). This study, therefore, examined the strength and cracking patterns performance of RC beams incorporated sea sand bonded externally with CFRP plate. Three groups of RC beams named control beam, RC beam incorporated with sea sand and bonded with CFRP plate, and normal RC beam bonded with CFRP plate were fabricated and tested under four-point bending load. Each group had three replicates, and the average was then taken.

2. Experimental Program

2.1 Materials

Cement, fine aggregate, coarse aggregate, CFRP plate, and epoxy adhesive are the materials used. Type I ordinary Portland cement (OPC) having 3.15 specific gravity and 2.2% loss of ignition and confirming the requirements prescribed in ASTM C150 [36] was utilized with the chemical composition shown in Table 1.

Table 1. OPC chemical compositions [37, 38]

Composition	SiO_2	Fe_2O_3	Al_2O_3	CaO	MgO	SO_3	C_3S	C_2S	C_3A
OPC (%) by mass	20.52	3.63	5.32	63.31	1.08	2.18	46.9	26.3	7.96

The concrete mix design was determined for achieving concrete grade 50 in accordance with BS 1881-124:2015 [39], which was then used throughout the study. Wooden formworks were utilized to mould the specimens. The water to cement ratio was 0.47. Crushed granite coarse aggregate with two sizes, nominal size of 10 mm and maximal size of 20 mm, was used together with fine aggregate (normal sand or sea sand) and OPC as the binding materials. The concrete mix design quantities are presented in Table 2. The sea sand (fine aggregate) was collected from a local west coast in the south of Kuala Lumpur, Port Dickson, Malaysia. The sand was passing through a 4.75 mm sieve and retailing on 75 mm.

Table 2. Concrete mix design quantities

Quantity	OPC (kg)	Water (kg/L)	w/c ratio	FA (kg)	CA (kg)	
					10 mm	20 mm
Per m^3 (to nearest 0.25 kg)	450	180	0.47	505	450	785

FA denotes fine aggregate (either normal sand or sea sand), and CA denotes the coarse aggregate

The CFRP plate utilized, as strengthening materials, was Selfix Carbofibre provided by the Exchem company with the cross-sections and mechanical properties shown in Table 3. CFRP plate was bonded externally to the concrete using epoxy adhesive. The type of adhesive was Sikadur 30 supplied by Sika Kimia (Sika Kimia Sdn. Bhd., Negeri Sembilan, Malaysia), which has the same brand as the CFRP plate. The structural epoxy was mixed accordingly based on the manufacturer's recommendation for the bonding application with

a mix ratio of 3:1 (epoxy-hardener). The epoxy adhesive was then applied before and after placing the CFRP in order to ensure that it fully in contact with concrete. Table 4 shows the adhesive epoxy mechanical properties.

Table 3. CFRP plate dimensions and mechanical properties

Plate	L (mm)	W (mm)	Thk (mm)	TS (MPa)	EM (GPa)	E (%)
CFRP	1400	50	1.2	3000	165	2.0

L denotes Length, W denotes width, Thk denotes thickness, TS denotes tensile strength, EM denotes elastic modulus, and E denotes elongation

Table 4. Mechanical properties of Epoxy

Type	BS (MPa)	TS (MPa)	EM (GPa)	CS (MPa)	E (%)
Epoxy	> 3	30	2	70	1.0

BS denotes bonding strength, TS denotes tensile strength, EM denotes elastic modulus, CS denotes compressive strength and E denotes elongation

2.2 Specimens preparation

Two batches of concrete mixes were prepared, namely normal concrete, sea sand concrete. Six cubes for each batch with characteristic strength of 50 MPa were cast and constructed following BS 8110 standard [40]. The mixture quantities are shown in Table 2. In this study, samples in the form of RC beams were prepared to examine the flexural and cracking behavior of sea sand RC beam strengthened externally, in the tension face, with CFRP. In addition, 2T10 as hunger bars and 2T12 mm as tension reinforcement bars having yield stress (f_y) and elastic modulus (E_s) of 460 MPa and 207 GPa, respectively, were utilized in each specimen. The link diameter of R6-300 having 250 MPa yield strength and 200 GPa elastic modulus was used, as shown in the cross-section A-A (Fig. 2). Three groups of RC beams with dimensions of 1600 mm length, 150 mm height and 100 mm width subjected to four-point bending load (P) were fabricated. The specimens were tested in accordance with ASTM D6272 [41] where the loading span is 1/3 of the support span. These three groups were control beam, RC beam incorporated with sea sand and bonded with CFRP plate, and normal RC beam bonded with CFRP plate. Each group had three replicates, and the average of the results was then taken. The curing process of the three RC beams was performed using the method of water retention by covering the sample for 28 days with wet rugs, as shown in Fig. 3.

The 1400 mm length and 1.20 mm thick CFRP plate is externally attached via the epoxy adhesive to the under-tension surface of the RC beam. For bonding purposes, the tension surface of the RC beams was exposed and roughened using an air tool hammer. The surface was then cleaned from any dust or any small concrete particles. Epoxy was carefully applied to the tension surface of the RC beams and into the surface of the CFRP plate. CFRP plate was then placed into the RC beam tension surface (Fig. 4) and pressed manually with hand homogenously throughout the bonded length to provide a firm bond between the CFRP plate and RC beam.

The specimens were cured for 28 days to achieve the target strength. The sample was then able to be set up and instrumented experimentally. The study aimed at the determination and observation of the ultimate load, deflection behavior, and cracking pattern and mode of failure of the RC beams. Therefore, linear variable differential transducer (LVDT), load cell, and data logger were the only instruments utilized. To measure the displacement under a four-point bending load, three LVDTs were placed on the beam tension face. The LVDTs are placed in the tension face of the RC beams on three different positions along the beam, which are at mid-span and at 300 mm from the middle for both sides. However, the data taken to plot the graph is for the LVDT placed on the mid-span. Fig. 5 shows the testing set-up and LVDTs locations.

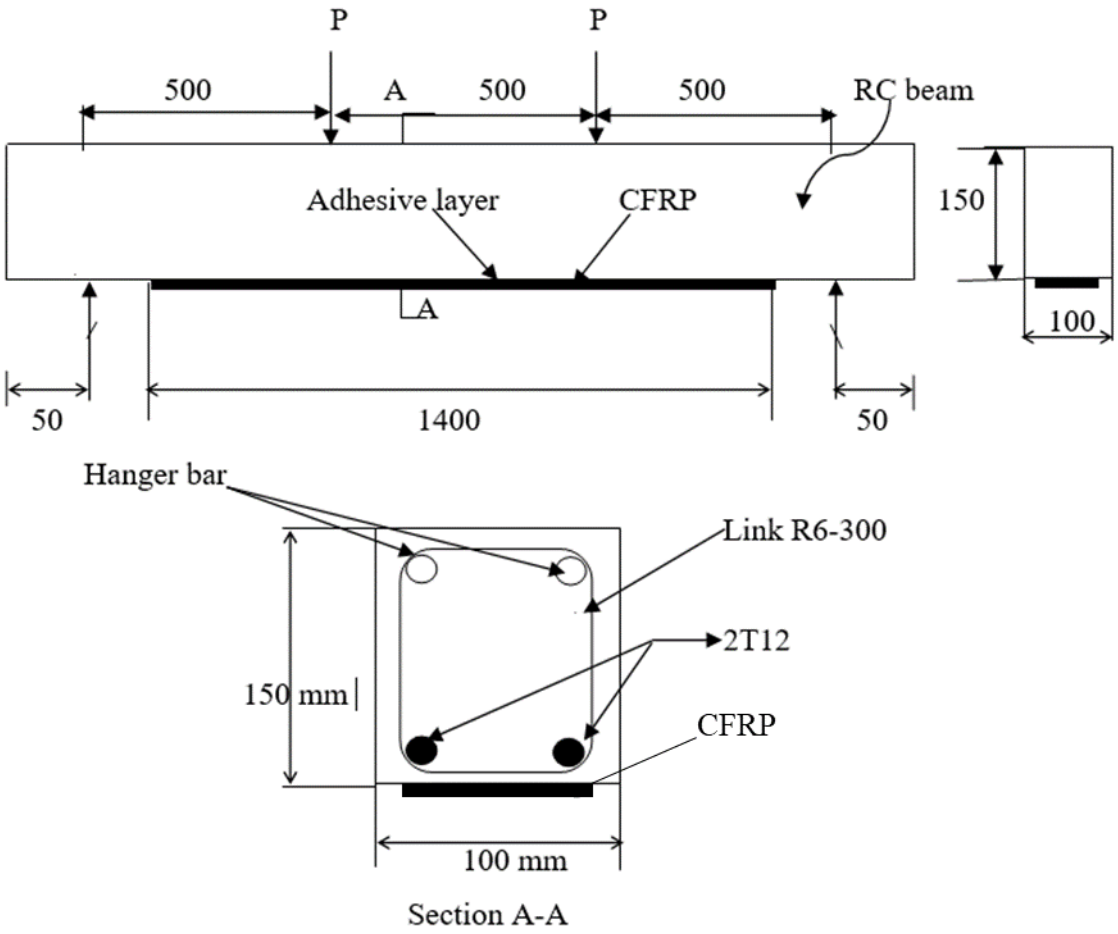

Fig. 2. RC beam bonded with CFRP configuration and load arrangement

Fig. 3. Casting and curing of RC beams

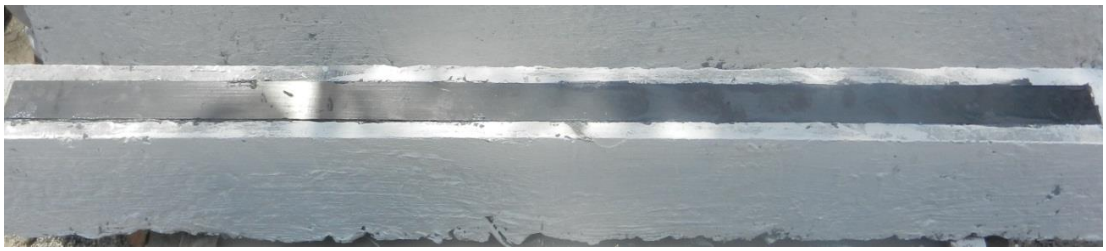

Fig. 4. CFRP bonded externally to RC beam

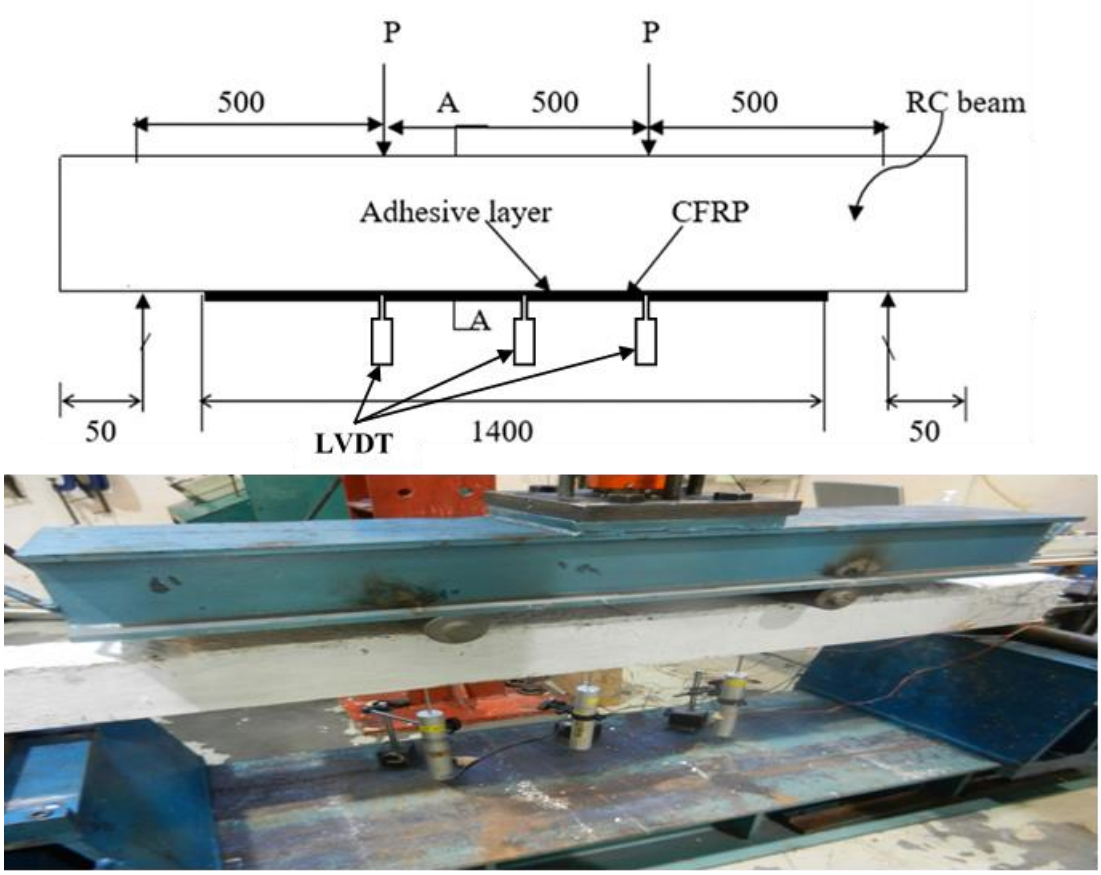

Fig. 5. Instrumentation and testing set-up (Schematic and laboratory diagrams)

3. **Finite element analysis (FEA)**

The nonlinear behavior of the beams was modeled using an FEA technique. For the study, the finite element modlling (FEM) kit Abaqus 6-13 [42] was used.

3.1 *Material Properties and Constitutive models***:**

a) Concrete

To describe concrete behaviour, the concrete damage plasticity model (CDP) implemented which some studies recommend simulating concrete behaviour because of its ability to deal with the 3D nonlinear inelastic behaviour of concrete as well as the confinement and damage mechanism, compressive, tensile, and plastic properties in the inelastic range [43-45]. Lubliner et al. [46] first introduced CDP then a development proposed by Lee and Fenves [47]. CDP can assume that there are two main failure modes are (1) tensile cracking and (2) compressive crushing. The behaviour of concrete in tension and compression is illustrated in Fig. 6.

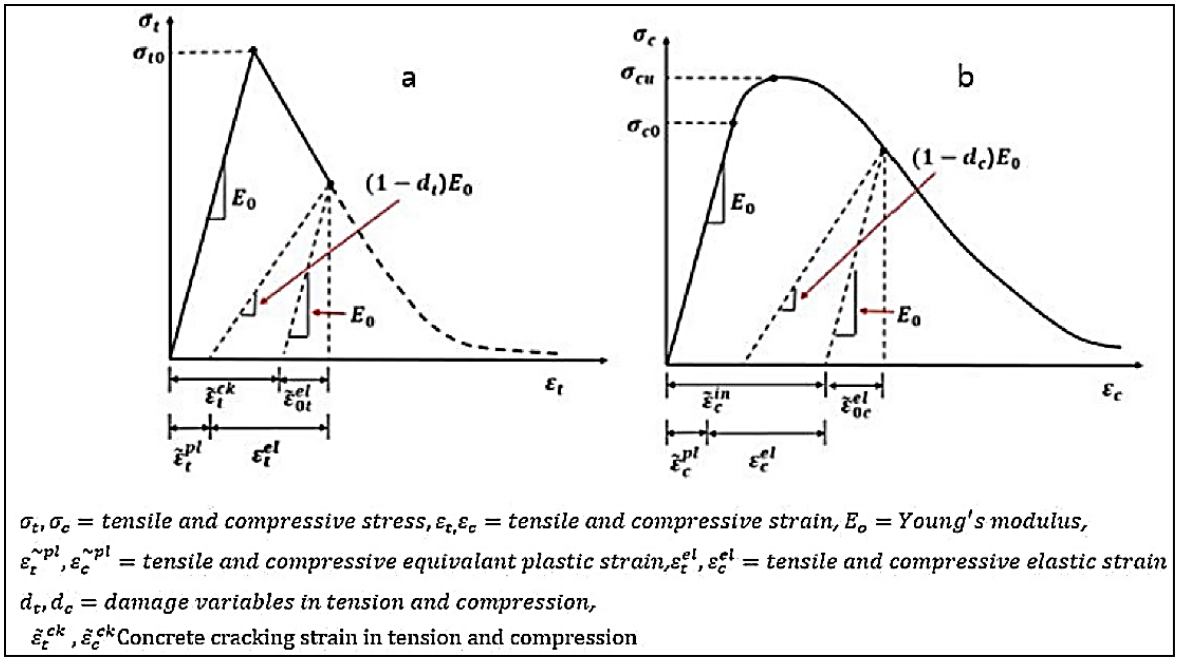

Fig. 6. Behavior of concrete under uniaxial load in (a) tension and (b) compression [48]

The CDP model in Abaqus 6-13 [42] consists of plastic behaviour, compressive behaviour, and tensile behaviour of concrete. For plastic behaviour, five parameters need to be defined which are: a) dilation angle (ψ) which is a result of volume strain over shear strain. Its value is ranged between 20^o – 40^o, b) the plastic potential eccentricity of concrete (ε), c) the ratio of compressive stress in the biaxial state to the compressive stress in the uniaxial state (σ_{b0}/σ_{c0}), d) the shape factor of the yielding surface in the deviatoric plane (K_c), and e) viscosity parameter. Table 5 summarizes the parameters and their defined values.

Table 5. plasticity model parameters

ψ	ε	σ_{b0}/σ_{c0}	K_c	Viscosity parameter
30	0.1	1.16	0.667	0.0055

Compressive behaviour of concrete in CDP model introduced according to Eurocode EN 1992-1-1 [49]. Which described in the following equations (Eqn. 1 – 4):

$$\sigma_c = f_c' \frac{k\eta - \eta^2}{1+(k-2)\eta} \quad (1)$$

Where :

$$k = 1.05E_c \frac{|\varepsilon_{c1}|}{f_c'} \quad (2)$$

$$\eta = \frac{\varepsilon_c}{\varepsilon_{c1}} \quad (3)$$

Where E_c is the modulus of elasticity of concrete:

$$E_c = 22\left[\frac{f_c'}{10}\right]^{0.3} \quad (4)$$

ε_{c1} is the strain corresponding to f_c', and ε_c is the concrete strain at a stress of σ_c. The equations proposed by Majewski [50] were used to find ε_{c1} and the ultimate strain ε_{cu} of the concrete as presented by the following equations (Eqn. 5 & 6)

$$\varepsilon_{c1} = 0.0014[2 - e^{-0.024f_c'} - e^{-0.14f_c'}] \quad (5)$$

$$\varepsilon_{cu} = 0.004 - 0.0011[1 - e^{-0.0215f_c'}] \quad (6)$$

The compression damage d_c is calculated as follow (Eqn. 8):

$$d_c = 1 - \frac{\sigma_c}{\sigma_{cu}} \quad (8)$$

For tension behaviour of concrete in CDP model according to relation presented in [51] (Eqn. 9):

$$\sigma_t = E_{cm}\varepsilon_t \quad if \quad \varepsilon_t \leq \varepsilon_{cr} \quad (9)$$

$$\sigma_t = f_t\frac{(\varepsilon_t)^{0.4}}{\varepsilon_{cr}} \quad if \quad \varepsilon_t \leq \varepsilon_{cr}$$

The tensile strength (f_t) can be obtained as follows [49] (Eqn. 10):

$$f_t = 0.3(f_{ck})^{2/3} \quad (10)$$

The tension damage d_t is calculated as follow(Eqn. 11):

$$d_t = 1 - \frac{\sigma_t}{\sigma_{t0}} \quad (11)$$

For an elastic definition, the Poisson ratio is assumed to be 0.2.

Several studies observed a reduction in modulus of elasticity when fine aggregate is replaced partly or fully with sea sand or seashells [5, 52-54]. Ming et al. [54] studied the mechanical properties of sea sand concrete. In their conclusion, they observed that the modulus of elasticity of sea sand concrete is 9% lower than normal concrete. They explained that hydration of cement leads sodium chloride to crystals and expand in volume causes internal

cracks in the concrete. Therefore, this study considers 9% reduction in modulus of elasticity for sea sand concrete.

b) Steel reinforcement

The steel was assumed to be an elastic–perfectly plastic material and identical in tension and compression. Material properties are described in section 2.2.

c) *CFRP*

The material properties of the elastic behaviour of CFRP are assumed to be isotropy. This assumption made based on the conclusion made by Obaidat et al. [55]. They concluded that assuming CFRP is isotropic leads to closer results to orthotropic assumption. Hence, define the material as isotropy reduce computation complexity so analysis time will be shorter.

d) Element selection and interaction

The model in this study was constructed using 3D elements. To model concrete and supports, an 8-node linear brick element with reduced interaction and hourglass control (C3D8R) was selected. Reinforcements were represented using a 2-node truss element with three degrees of freedom at each node (T3D2). The CFRP material was modeled using 4-node shell with reduced integration and hourglass control (S4R). The fine mesh was applied to ensure results accuracy.

The interaction between concrete and reinforcement is assumed to be a perfect bond by applying the "Embedded region". Two types of interaction were implemented to study their effect on beam load capacity:

i. Perfect bond: This definition means that CFRP is firmly adhered to concrete and assures that the relationship between concrete and CFRP does not lead to a failure. This interaction is applied by defining the "Tie" constrain between concrete and CFRP.
ii. Cohesive-behaviour contact: the concept is to model the adhesive contact properties to define the interaction between concrete and CFRP. The type of interaction is "Surface-surface contact" where the concrete is the master part and CFRP is the slave. Contact properties is cohesive-behaviour, Table 6 shows Epoxy properties defined in Abaqus.

Table 6. Epoxy properties defined in Abaqus

E	G	$t_{Adhesive}$	Knn= E/ $t_{Adhesive}$	Kss= G/ $t_{Adhesive}$	Ktt= G /$t_{Adhesive}$

2 GPa	0.665 GPa	0.1mm	20	6.65	6.65

E denotes elastic modulus, G denotes shear modulus, tAdhesive denotes adhesive thickness, Knn,Kss,Ktt denotes stiffness Coefficients

e) Boundary conditions and model configuration

Boundary conditions for supports were applied "Pin" for support 1 and roller for support 2. For applied load, displacement concept adopted where the two point-loads are constrained by "Coupling constraint" to a master point at the centre of the beam to ensure simultaneous movement. Fig. 7 illustrates the boundary conditions and model configuration.

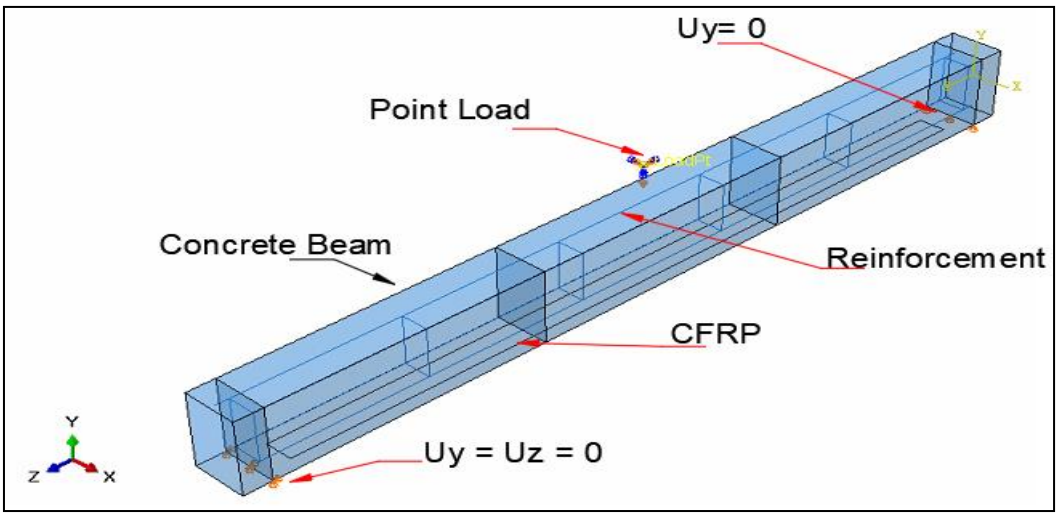

Fig. 7. Boundary conditions and model configuration

4. Results and discussion

4.1 Compressive strength test

The first part of the experiment examined the concrete strength to meet the specified strength (50 MPa). The result of the cube test at 7 and 28 days of curing is shown in Fig. 8. The result indicates that the sea sand concrete inherited early high compressive strength at seven days, contrasting with normal sand concrete. However, the compressive strength at 28 days was found to be mostly the same (50.23 MPa for normal sand concrete and 49.63 MPa for sea sand concrete). The early high strength that sea sand concrete achieved is due to the combination of chlorides that contain in the sea sand with cement (OPC). This finding is in line with the literature reviewed by Dhondy, et al. [4] and Xiao, et al. [5].

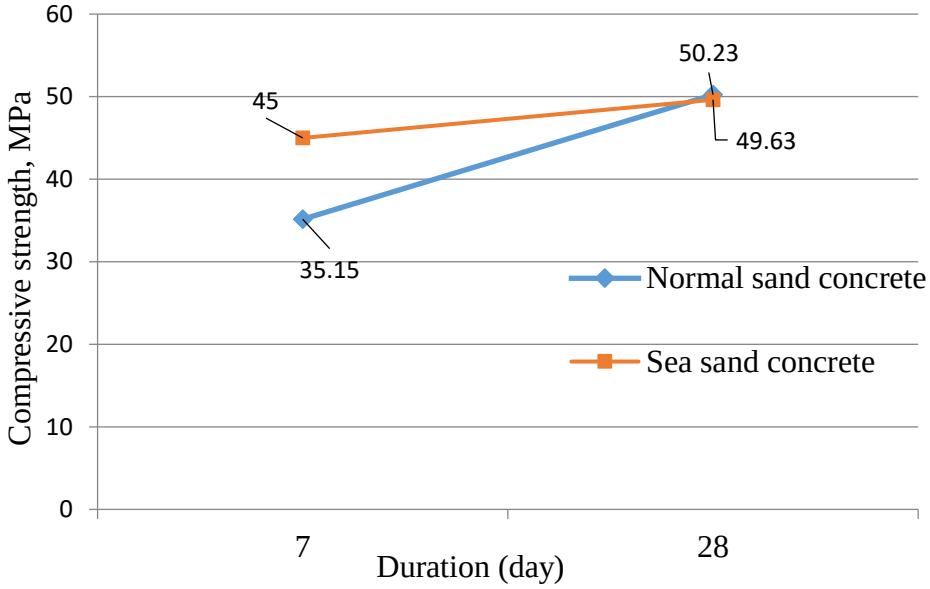

Fig. 8. Compressive strength test results

4.2 Deflection performance

Fig. 9 reveals the graph of load vs. deflection at the mid-span of the three tested beams (control beam, RC beam incorporated sea sand and bonded with CFRP (sea sand beam), and RC beam bonded with CFRP (normal sand beam) subjected to static four-point bending load. It can be seen that the control RC beam behaves approximately linearly between the applied load and deflection until it reached the maximum applied load of 25.7 kN and optimal deflection of 15.6 mm. However, the RC beam strengthened with CFRP behaves linearly between the applied load and deflection until it reached the maximum applied load of 31.7 kN and optimal deflection of 6.3 mm while the RC beam incorporated sea sand and externally bonded with CFRP behaves gradually increasing until it reached the maximum applied load of 26.1 kN and maximum deflection of 6.8 mm. Based on the result obtained it can be seen that the strength performance of RC beam incorporated with sea sand and externally bonded with CFRP is 5.50% greater than the control beam strength, which indicates good performance. In contrast, the normal beam bonded with the CFRP plate shows high strength performance compare to the control and sea sand RC beams.

Based on the load-deflection relationship of the beams at mid-span, the more strength capacity is the beam, the more improvement of deflection can be obtained. Besides, it can be observed that the improvement in deflection capacity indicated an increase in beam stiffness strengthened by the CFRP plate compared to the unstrengthened control beam. Also, it can be revealed that the stiffness of the RC beam incorporated with sea sand and

bonded externally with CFRP plate is lower than the normal RC beam bonded externally with CFRP plate.

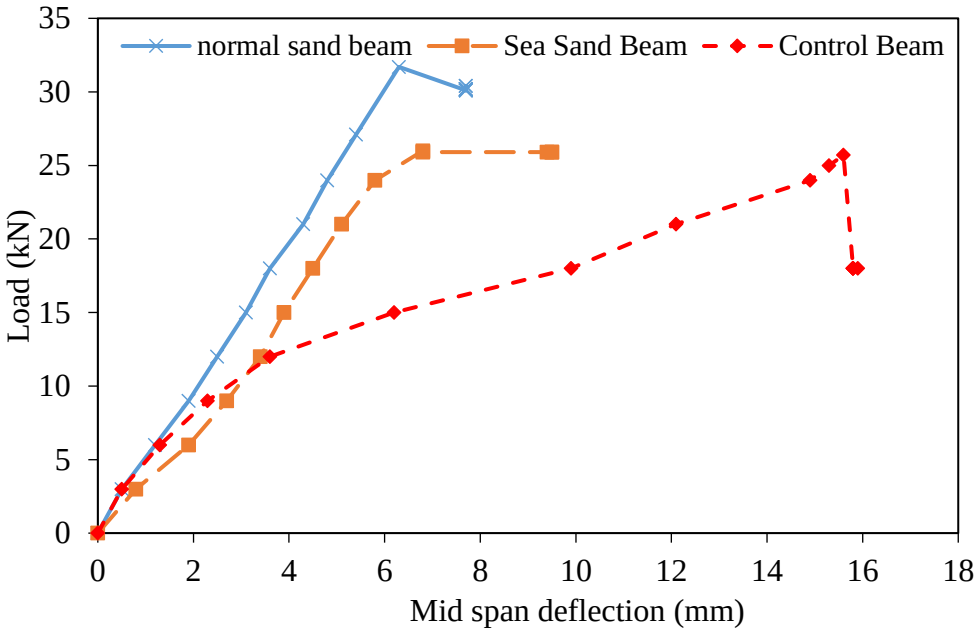

Fig. 9. Load vs. deflection relationship

In general, strengthening reinforced concrete beams with CFRP plate improved the load-deflection behaviour of the beams. Additionally, both RC beams that strengthened with CFRP plate shown better deflection behaviour than the unstrengthened control beam. The differences between the two RC beams strengthened were the amount of deflection that can be standing by the strengthened beam.

4.3 Cracking patterns

Cracking patterns is an important parameter in structure elements which required observation and measurement during experimental work. Cracks can be either flexural or shear cracks. The flexural crack pattern is almost a vertical crack and perpendicular to the principal stress, while the shear crack is the inclined cracks that approach the shear region. Fig. 10 shows a view of crack patterns on the side of the three beams tested under the static loading. It can be seen from the side view that at the beginning of the applied load, flexural cracks were formed in all of them. However, the cracks began to appear to be like shear cracks as the applied load increased.

Based on the observation and from Fig. 10, the RC beam mixed with sea sand strengthened with CFRP started to crack when the applied load reached the value of 3.3 kN with deflection of 1 mm, while the normal beam strengthened with CFRP started to

crack when the applied load reached the value of 9.4 kN with deflection of 2 mm. However, the initial crack of the unstrengthened control beam was at an applied load of 0.8 kN with deflection of 1 mm. as a result, at those points of initial cracks of each beam, the concrete is exceeding the yield strength. When the applied load reached the maximum strength, the loads started to decrease, and the cracks became bigger.

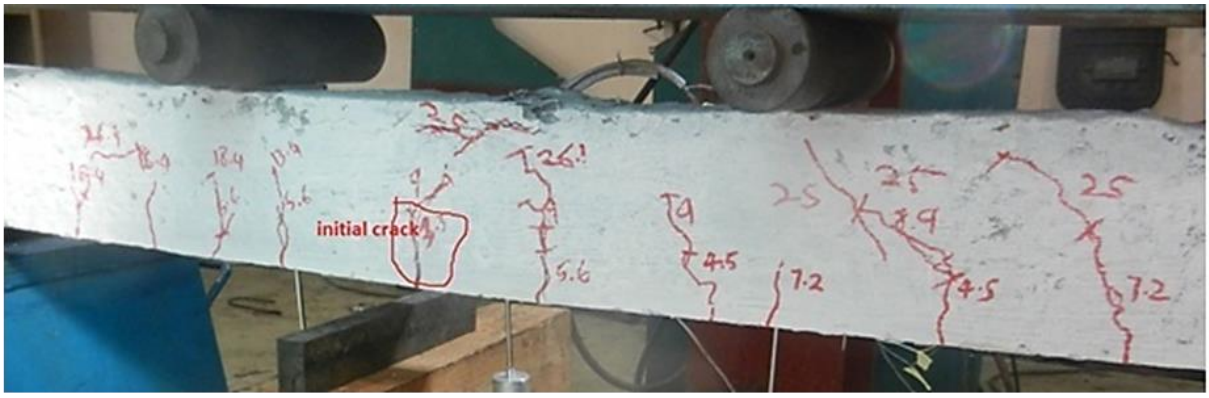

(a)

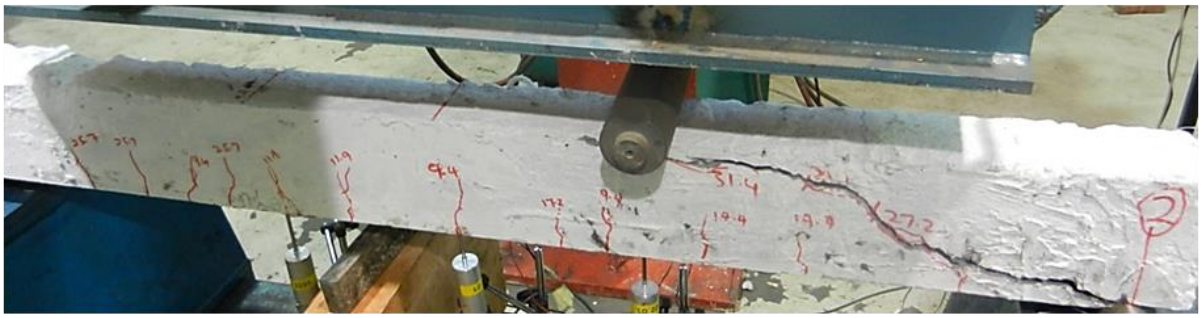

(b)

(c)

Fig. 10. Cracking patterns A) Control beam, B) Normal sand beam bonded with CFRP , C) Sea sand beam bonded with CFRP

4.4 Failure modes

Additionally, Fig. 11(a, b) shows the plate debonded with concrete. It can be seen that the cracks increase toward the region between the CFRP and concrete. However, as the cracks approach into the shear region, the bonding strength between CFRP and concrete

started to decrease and suddenly debonded the plate from the concrete, as shown in Fig. 11b. On the other hand, Fig. 12 shows the failure of the unstrengthened control beam. It can be seen that the control beam with no bonding fails with concrete crushing at the mid-span of the beam.

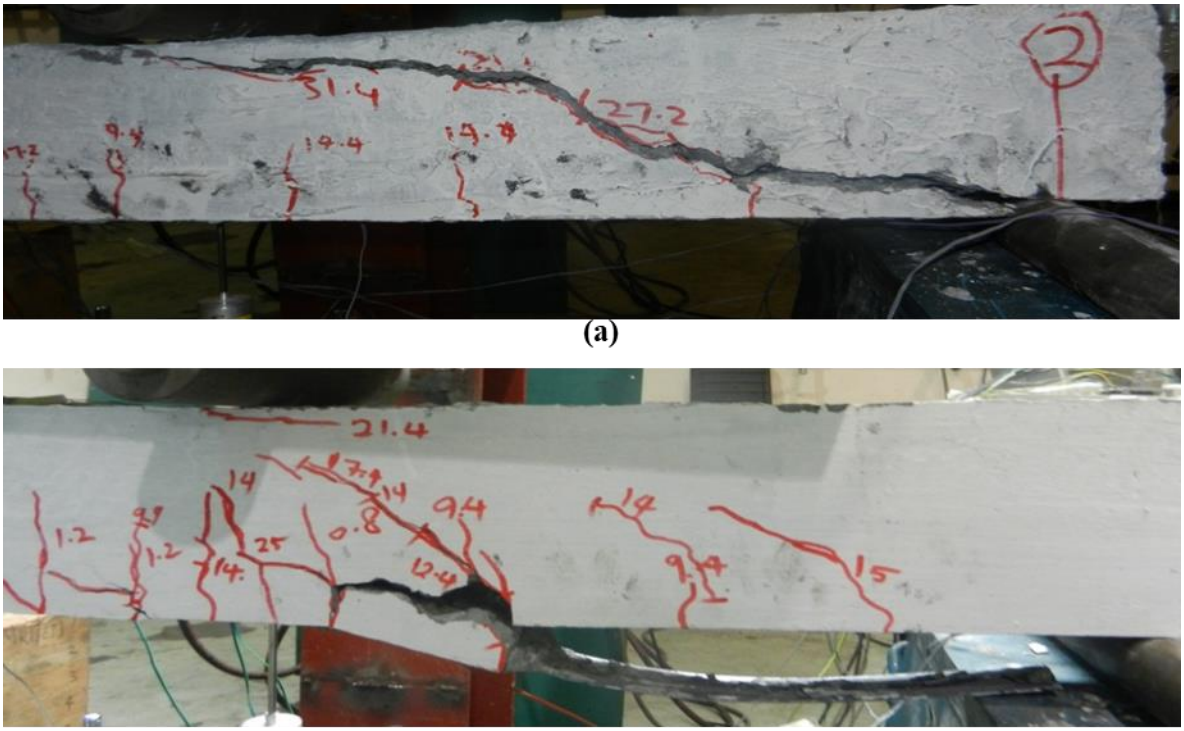

(a)

(b)

Fig. 11. Failure mode of a) Normal sand RC beam bonded with CFRP , B) Sea sand RC beam bonded with CFRP

Fig. 12. Failure mode of control beam

Table 7 shows the crack's behaviour and failure modes of the tested specimens. The spacing between the cracks was determined at the tension side of the beams. It is observed that the spacing of the cracks for the beam bonded externally with CFRP plate was on the average of 30 mm, while the spacing of the cracks on the tension side of the control beam without externally bonding with CFRP plate was on the average of 55 mm.

As a result, the spacing of the cracks for the beams bonded externally with CFRP plate was less than the spacing of the cracks of the control beam without bonding CFRP plate. The rigidity of the refined concrete will in other words influence the cracking behaviour of the beams bonded externally with CFRP. Additionally, it can be seen that strengthening the RC beam with CFRP at the tension side may cause a reduction of cracks spacing. The spacing range from 12 – 57 mm for the normal sand beam strengthened with CFRP and varied from 14 – 59 mm for the sea sand beam strengthened with CFRP plate and varied from 27 – 84 mm for the control beam, as shown in Table 7. So, we can say that the average spacing for beams strengthened with CFRP plate was approximately 29 % to 55 % lower than the average spacing of the control beam.

Table 7. Cracking behaviour and failure Modes of the tested RC beams

Beams	Ultimate Load (kN)	Number of cracks			Range crack spacing(mm)	Average spacing(mm)	Failure mode
		Shear	CMR	Total			
Normal Sand beam with CFRP	31.7	6	4	10	12 – 57	27	PED
Sea Sand beam with CFRP	26.1	5	8	13	14 – 59	33	PED
Control beam	25.7	7	5	12	27 – 84	55	CR

[CMR – Constant Moment Region; CR – Concrete Crushing; PED – Plate End Debonding]

4.5 Finite element analysis Results

4.5.1 Load-Deflection comparison

The load-deflection curves obtained for the control beam and strengthened beams from experiments and FEM analysis are shown in Fig. 13. Two different bonding models for CFRP and concrete were used.

There is good agreement between FEM and experimental results in terms of maximum load capacity for all three specimens. However, there is a significant difference in deflection between experimental and FE results. This difference can be related to human error during experimental measurements or as described by Obaidat et al. [55] that perfect bond assumption may produce stiffer models. Even though the deflection in the three graphs differs, the load capacity results showed agreement ranged from 79.06% - 93.8%.

The effect of interaction type seems insignificant when observing FE results in Fig. 13 (a, b). the perfect bond assumption gives similar results as cohesive-behaviour contact. Therefore, implement either tie or cohesive-behaviour contact will lead to having similar results. However, in such cases “tie” constraint is favourable regarding its simplicity and time inexpensive analysis.

Beam's ultimate load capacity is taken after the first drop in the graph. In Fig. 13 (a, b) both models over-estimate the beam stiffness and continue to increase the load after a slight drop. This drop starts at values equivalent to experimental ones. The continuity beam stiffness can be attributed to CFRP resistance. The experimental and FEM simulated ultimate load capacity of the beams are compared in Table 8.

Table 8. Comparison between experimental and FEM simulated ultimate load capacity of the beams

Model	Ultimate Load (kN)		FE/Exp ratio
	Experimental	FEM	
Control Beam	25.7	30.365	1.265
Normal sand beam bonded with CFRP (Perfect bond)	31.7	33.805	1.066
Normal sand beam bonded with CFRP (Cohesive-behaviour contact)		34.32	1.083
Sea sand beam bonded with CFRP (Perfect bond)	26.1	32.27	1.246
Sea sand beam bonded with CFRP (Cohesive-behaviour contact)		32.76	1.245

From the table, it can be notice that sea sand beams bonded with CFRP are higher than control beam. These results agreed with experimental observation. It shows that CFRP strengthening improved the performance of the sea sand concrete beam. In contrast, normal sand beam bonded with CFRP give the highest ultimate load.

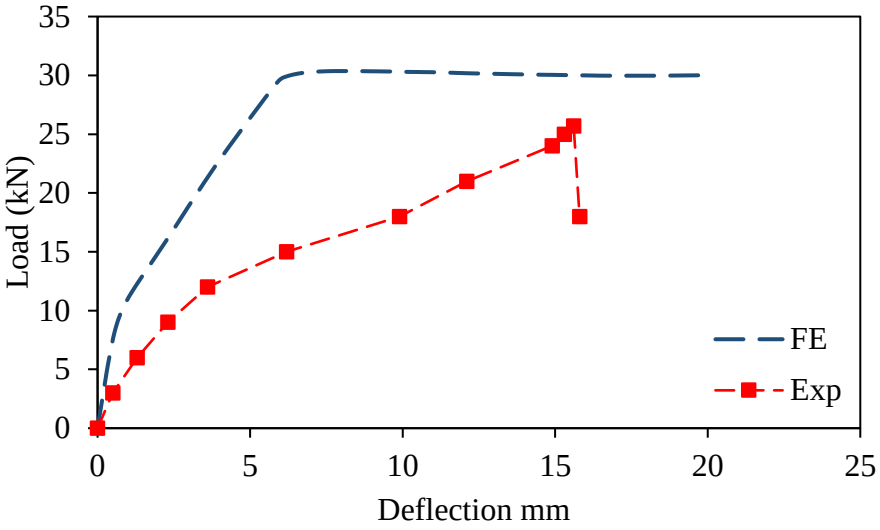

(a)

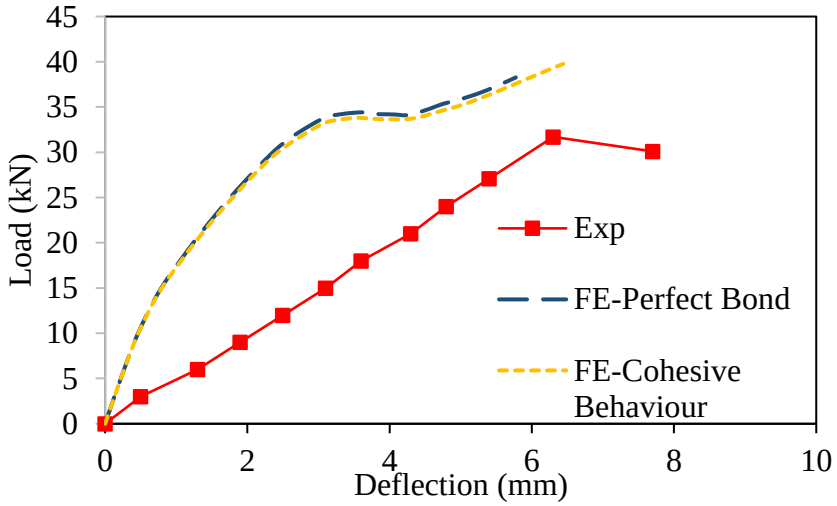

(b)

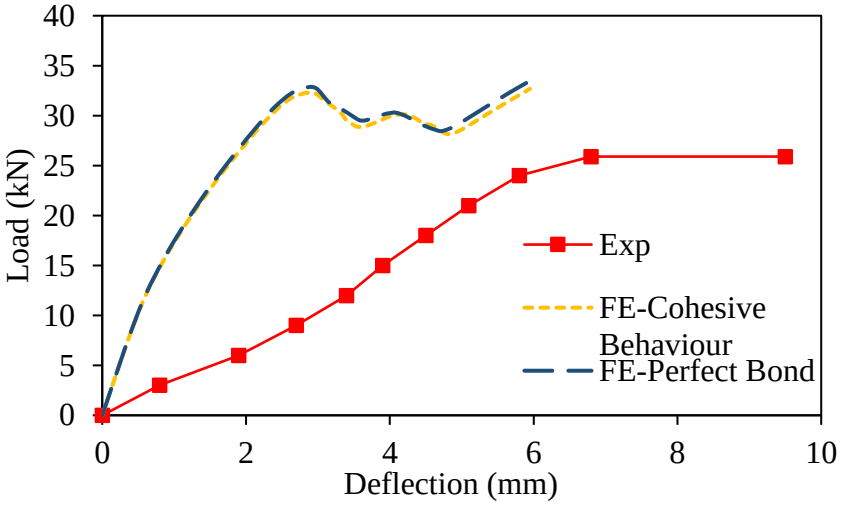

(c)

Fig. 13. Load-Deflection curve obtained from experiment and FE: a) Control Beam, b) Normal sand beam bonded with CFRP , c) Sea sand beam bonded with CFRP

4.5.2 Crack pattern

The crack pattern is an important parameter to test the model's ability to capture the mechanism of fracture of the beam. Since this study focuses on the performance of sea sand beam bonded with CFRP. Then, a crack pattern for sea sand beam bonded with CFRP is presented in this section and compared with the experimental results. On the other hand, the crack pattern of thenormal sand beam bonded with CFRP is presented to compare interaction model's ability to show crack development.

Cracks forming at the material integration stage are not included in the concrete damaged plasticity model. However, in order to achieve graphical simulation of cracking patterns on the concrete structure, the idea of an effective crack direction can be introduced. Various parameters for the description of the direction of cracking may be used within the context of scalar-damage plasticity. According to Lubliner et. al., [46], cracking starts at points where the equivalent tensile plastic strain exceeds zero and the maximum main plastic strain is positive.

Fig. 14 demonstrates that both interaction models are able to capture crack patterns of the specimens. Cohesive-behaviour contact showed quite a better crack pattern than perfect bond however this advantage is not remarkable.

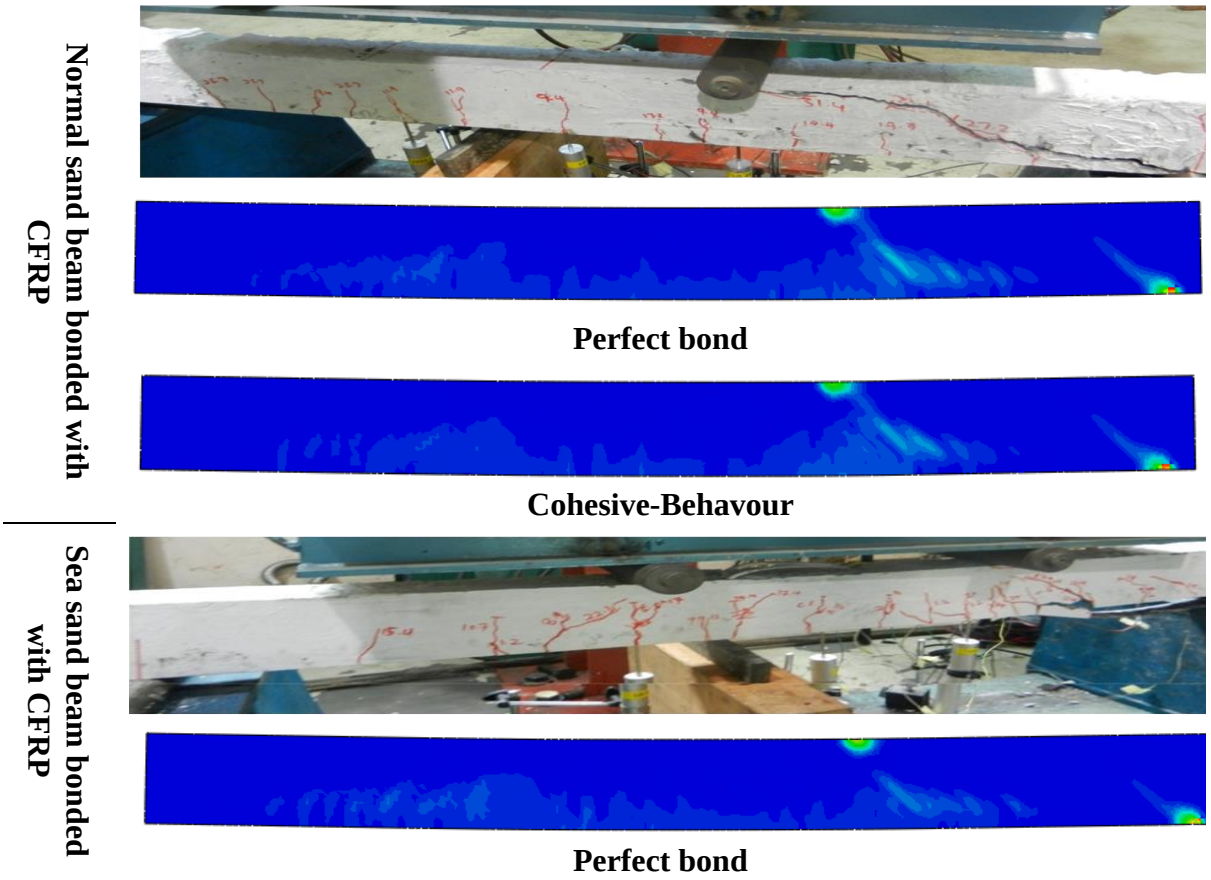

Cohesive-Behaviour

Fig. 2. Crack pattern of FE models a) Normal sand RC beam bonded with CFRP , B) Sea sand RC beam bonded with CFRP

4.5.3 Failure mode

Since the perfect bond model excludes bond fracture, it is unable to model the debonding fracture mode observed in the experiments. On the other side, the cohesive model will reflect debonding. Debonding fracturing happened while the cohesive bond model was used. This is illustrated in Fig. 15.

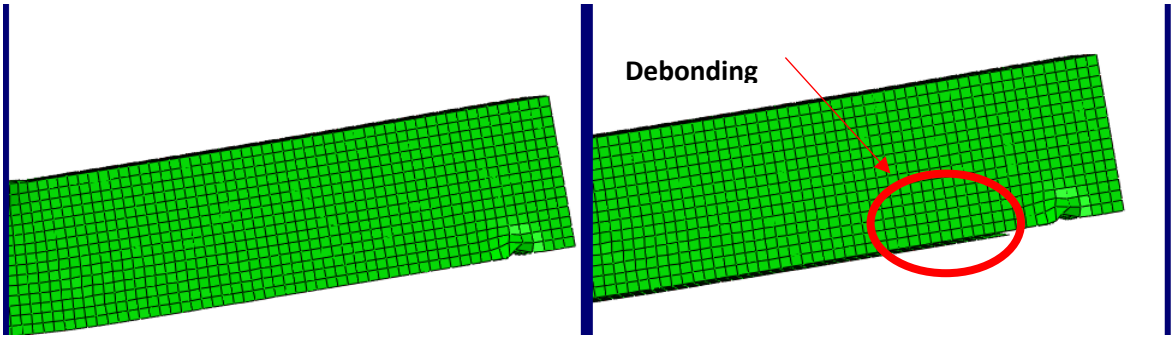

Perfect bond **Cohesive-Behaviour**

Fig. 3. Failure mode of FE models a) Normal sand RC beam bonded with CFRP , B) Sea sand RC beam bonded with CFRP

5. Conclusion

CFRP plate increases the stiffness capacity of the RC beam, which increases the strength performance of that beam. However, several conclusions can be made to the strength performance and cracking patterns behaviour of the RC beam incorporated sea sand and bonded with the CFRP plate.

1. Based on the compressive strength results, it can be concluded that the concrete was not affected by mixing the sea sand as fine aggregate as the compressive strength was met the target strength after 28 days.
2. Based on load-deflection behaviour, it can be concluded that RC Beams bonded externally with CFRP plate had higher stiffness compared to the control beam without bonding.
3. CFRP plates are suitable for strengthening materials that can improve the sea sand RC beam strength or normal sand RC beam.

4. RC beams bonded externally with CFRP plate failed in plate end debonding (PED) of the CFRP plate while the control beam without bonding failed in concrete crushing at the mid-span of the beam.
5. Strengthening the RC beam with CFRP can improve the cracking performance of the concrete beam.
6. Finite element simulation showed a very acceptable results compared to the experimental results.

Funding:

Acknowledgments: In the form of the re-search project no. 2020/01/16810, this project was funded by the Deanship of scientific research of the University of Prince Sattam bin Abdulaziz (Saudi Arabia). The authors would like to thank Universiti Teknologi MARA (UiTM) for helping on conducting the experiment and special thanks to Universiti Teknologi Petronas (UTP) for supporting the writing.

References

[1] L.J.W. Bing Quan Sun, Chao He Chen, Hong Wang, A New Technique to Manufacture Desalinated Sea Sand Concrete and its Properties, Advanced Materials Research Volumes 250 - 253 (May, 2011) 283-290.
[2] Z. Guoliang, L. Junzhe, C. Jianbin, H. Zhimin, Study on the properties of sea sand concrete, Mechanic Automation and Control Engineering (MACE), 2011 Second International Conference on, 2011, pp. 3584-3587.
[3] Z. Dong, G. Wu, H. Zhu, X.-L. Zhao, Y. Wei, H. Qian, Flexural behavior of seawater sea-sand coral concrete–UHPC composite beams reinforced with BFRP bars, Constr. Build. Mater. 265 (2020) 120279.
[4] T. Dhondy, A. Remennikov, M.N. Shiekh, Benefits of using sea sand and seawater in concrete: a comprehensive review, Australian Journal of Structural Engineering 20(4) (2019) 280-289.
[5] J. Xiao, C. Qiang, A. Nanni, K. Zhang, Use of sea-sand and seawater in concrete construction: Current status and future opportunities, Constr. Build. Mater. 155 (2017) 1101-1111.
[6] A. Younis, U. Ebead, A. Nanni, A perspective on seawater/FRP reinforcement in concrete structures, Proceedings of the Ninth International Structural Engineering and Construction Conference, Resilient Structures and Sustainable Construction, ISEC Press Valencia, Spain, 2017, pp. St-38.
[7] S. Li, Experiment studies on the shear performance of sea sand concrete beam with BFRP tendons, Master degree thesis (2014).
[8] J. Teng, T. Yu, J. Dai, G. Chen, FRP composites in new construction: current status and opportunities, Proceedings of the 7th national conference on FRP composites in infrastructure, 2011.
[9] J. Teng, Performance enhancement of structures through the use of fibre-reinforced polymer (FRP) composites, (2014).
[10] P. Feng, J. Wang, X. Zhang, L. Ye, Q. Yue, Development and innovation on combining FRP and sea sand concrete for structures, Chinese.] Fiber Reinf. Plast./Compos 12(1) (2014) 13-18.
[11] D. Zhang, Y. Zhao, W. Jin, T. Ueda, H. Nakai, Shear strengthening of corroded reinforced concrete columns using pet fiber based composties, Eng. Struct. 153 (2017) 757-765.
[12] L.Z. Li, Z.L. Wu, J.T. Yu, X. Wang, J.X. Zhang, Z.D. Lu, Numerical simulation of the shear capacity of bolted side-plated RC beams, Eng. Struct. 171 (2018) 373-384.

[13] N.I. Rahim, B.S. Mohammed, A. Al-Fakih, M.M.A. Wahab, M.S. Liew, A. Anwar, Y.H.M. Amran, Strengthening the Structural Behavior of Web Openings in RC Deep Beam Using CFRP, Materials 13(12) (2020) 2804.
[14] A. Al-Nini, E. Nikbakht, A. Syamsir, N. Shafiq, B.S. Mohammed, A. Al-Fakih, W. Al-Nini, Y.H.M. Amran, Flexural Behavior of Double-Skin Steel Tube Beams Filled with Fiber-Reinforced Cementitious Composite and Strengthened with CFRP Sheets, Materials 13(14) (2020) 3064.
[15] H.L. Lye, B.S. Mohammed, M.S. Liew, M.M.A. Wahab, A. Al-Fakih, Bond behaviour of CFRP-strengthened ECC using Response Surface Methodology (RSM), Case Stud. Constr. Mater. 12 (2020) e00327.
[16] Z. Dong, G. Wu, Y. Xu, Experimental study on the bond durability between steel-FRP composite bars (SFCBs) and sea sand concrete in ocean environment, Constr. Build. Mater. 115 (2016) 277-284.
[17] T. Meikandaan, R. Murthy, Study of damaged RC beams repaired by bonding of CFRP laminates, Technology 8(2) (2017) 470-486.
[18] A. Remennikov, M. Goldston, M.N. Sheikh, Impact performance of concrete beams externally bonded with carbon FRP sheets, Mechanics of Structures and Materials: Advancements and Challenges–Hao & Zhang (Eds). Conference: Proceedings of the 24th Australian Conference on the Mechanics of Structures and Materials (ACMSM24), At Perth, Australia, 2016, pp. 1695-1699.
[19] R. Wight, M. Green, M. Erki, Prestressed FRP sheets for poststrengthening reinforced concrete beams, Journal of composites for construction 5(4) (2001) 214-220.
[20] A. Hosny, H. Shaheen, A. Abdelrahman, T. Elafandy, Performance of reinforced concrete beams strengthened by hybrid FRP laminates, Cement and Concrete Composites 28(10) (2006) 906-913.
[21] N.F. Grace, G. Sayed, A. Soliman, K. Saleh, Strengthening reinforced concrete beams using fiber reinforced polymer (FRP) laminates, ACI Structural Journal-American Concrete Institute 96(5) (1999) 865-874.
[22] Y. Zhou, Y. Zheng, J. Pan, L. Sui, F. Xing, H. Sun, P. Li, Experimental investigations on corrosion resistance of innovative steel-FRP composite bars using X-ray microcomputed tomography, Composites Part B: Engineering 161 (2019) 272-284.
[23] T. Liu, X. Liu, P. Feng, A comprehensive review on mechanical properties of pultruded FRP composites subjected to long-term environmental effects, Composites Part B: Engineering 191 (2020) 107958.
[24] J.-G. Dai, H. Yokota, M. Iwanami, E. Kato, Experimental Investigation of the Influence of Moisture on the Bond Behavior of FRP to Concrete Interfaces, Journal of Composites for Construction 14(6) (2010) 834-844.
[25] Y.H. Mugahed Amran, R. Alyousef, R.S.M. Rashid, H. Alabduljabbar, C.-C. Hung, Properties and applications of FRP in strengthening RC structures: A review, Structures 16 (2018) 208-238.
[26] Y. Liu, T. Tafsirojjaman, A.U.R. Dogar, A. Hückler, Bond behaviour improvement between infra-lightweight and high strength concretes using FRP grid reinforcements and development of bond strength prediction models, Constr. Build. Mater. 270 (2021) 121426.
[27] Y. Liu, T. Tafsirojjaman, A.U.R. Dogar, A. Hückler, Shrinkage behavior enhancement of infra-lightweight concrete through FRP grid reinforcement and development of their shrinkage prediction models, Constr. Build. Mater. 258 (2020) 119649.
[28] T. Tafsirojjaman, S. Fawzia, D. Thambiratnam, X.-L. Zhao, Behaviour of CFRP strengthened CHS members under monotonic and cyclic loading, Composite Structures 220 (2019) 592-601.
[29] W. Wenwei, L. Guo, Experimental study and analysis of RC beams strengthened with CFRP laminates under sustaining load, International Journal of Solids and Structures 43(6) (2006) 1372-1387.
[30] T. Norris, H. Saadatmanesh, M.R.J.J.o.s.e. Ehsani, Shear and flexural strengthening of R/C beams with carbon fiber sheets, 123(7) (1997) 903-911.
[31] M.R. Aram, C. Czaderski, M. Motavalli, Debonding failure modes of flexural FRP-strengthened RC beams, Composites Part B: Engineering 39(5) (2008) 826-841.

[32] N. Salleh, A.R. Mohd Sam, J. Mohd Yatim, Flexural behavior of GFRP RC beam strengthened with carbon fiber reinforced polymer (CFRP) plate: Cracking behavior, Appl. Mech. Mater., Trans Tech Publ, 2015, pp. 610-616.
[33] J. Teng, J. Yao, Plate end debonding failures of FRP-or steel-plated RC beams: A new strength model, (2005).
[34] A. Mukherjee, S.J. Arwikar, Performance of externally bonded GFRP sheets on concrete in tropical environments. Part I: Structural scale tests, Composite Structures 81(1) (2007) 21-32.
[35] C. F, Experimental performances of RC beams strengthened with FRP materials, Construction and Building Materials 24(9) (2010) 1547-1559.
[36] ASTM C150 / C150M-17, Standard Specification for Portland Cement, ASTM International, West Conshohocken, PA, 2017, pp. 1-7.
[37] A. Al-Fakih, B.S. Mohammed, M.S. Liew, W.S. Alaloul, Physical properties of the rubberized interlocking masonry brick, Int. J. Civ. Eng. Technol. 9(6) (2018) 656-664.
[38] A. Al-Fakih, B.S. Mohammed, M.S. Liew, W.S. Alaloul, M. Adamu, V.C. Khed, M.A. Dahim, H. Al-Mattarneh, Mechanical behavior of rubberized interlocking bricks for masonry structural applications, Int. J. Civ. Eng. Technol. 9(9) (2018) 185-193.
[39] B. 1881, Testing Concrete. Methods for analysis of hardened concrete, BSI London, UK, 2015.
[40] B. BS, Part 1, Code of practice for design and construction, structural use of concrete, London: British Standards Institution (1997).
[41] A.D.-. 17e1, Standard Test Method for Flexural Properties of Unreinforced and Reinforced Plastics and Electrical Insulating Materials by Four-Point Bending, ASTM international, West Conshohocken, PA, 2017.
[42] ABAQUS 6.13-4, Dassault Systèmes Simulia Corp., Providence, RI., (2013).
[43] M. Hafezolghorani, F. Hejazi, R. Vaghei, M.S.B. Jaafar, K. Karimzade, Simplified Damage Plasticity Model for Concrete, Structural Engineering International 27(1) (2017) 68-78.
[44] A. Raza, Q.u.Z. Khan, A. Ahmad, Numerical Investigation of Load-Carrying Capacity of GFRP-Reinforced Rectangular Concrete Members Using CDP Model in ABAQUS, Advances in Civil Engineering 2019 (2019) 1745341.
[45] A. Raza, A.u. Rehman, B. Masood, I. Hussain, Finite element modelling and theoretical predictions of FRP-reinforced concrete columns confined with various FRP-tubes, Structures 26 (2020) 626-638.
[46] J. Lubliner, J. Oliver, S. Oller, E. Oñate, A plastic-damage model for concrete, International Journal of Solids and Structures 25(3) (1989) 299-326.
[47] J. Lee, G.L. Fenves, Plastic-Damage Model for Cyclic Loading of Concrete Structures, Journal of Engineering Mechanics 124(8) (1998) 892-900.
[48] W. Li, C.K.Y. Leung, Shear Span–Depth Ratio Effect on Behavior of RC Beam Shear Strengthened with Full-Wrapping FRP Strip, Journal of Composites for Construction 20(3) (2016) 04015067.
[49] Eurocode 3: Design of steel structures - Part 1-1: General rules and rules for buildings, Eurocode 3: Design of Steel Structures, Part 1.2: General Rules, Structural Fire Design (1995).
[50] S. Majewski, The Mechanics of Structural Concrete in Terms of Elasto-Plasticity, Publishing House of Silesian University of Technology (0000).
[51] T. Wang, T.T.C. Hsu, Nonlinear finite element analysis of concrete structures using new constitutive models, Computers & Structures 79(32) (2001) 2781-2791.
[52] E.I. Yang, M.Y. Kim, H.G. Park, S.T. Yi, Effect of partial replacement of sand with dry oyster shell on the long-term performance of concrete, Constr. Build. Mater. 24(5) (2010) 758-765.
[53] E.I. Yang, S.T. Yi, Y.M. Leem, Effect of oyster shell substituted for fine aggregate on concrete characteristics: Part I. Fundamental properties, Cem. Concr. Res. 35(11) (2005) 2175-2182.
[54] C.U.I. Ming, M.A.O. Ji-Ze, J.I.A. Dao-Guang, L.I. Ben, Experimental Study on Mechanical Properties of Marine Sand and Seawater Concrete, 2014 International Conference on Mechanics and Civil Engineering (icmce-14), Atlantis Press, 2014, pp. 106-111.

[55] Y.T. Obaidat, S. Heyden, O. Dahlblom, The effect of CFRP and CFRP/concrete interface models when modelling retrofitted RC beams with FEM, Composite Structures 92(6) (2010) 1391-1398.